

East Tennessee State University

Digital Commons @ East Tennessee State University

ETSU Faculty Works

Faculty Works

5-17-2018

Highly Stable [C₆₀AuC₆₀]^{+/-} Dumbbells

Marcelo Goulart

Institut fur Ionenphysik und Angewandte Physik

Martin Kuhn

Institut fur Ionenphysik und Angewandte Physik

Paul Martini

Institut fur Ionenphysik und Angewandte Physik

Lei Chen

Institut fur Ionenphysik und Angewandte Physik

Frank Hagelberg

East Tennessee State University, hagelber@etsu.edu

See next page for additional authors

Follow this and additional works at: <https://dc.etsu.edu/etsu-works>

Citation Information

Goulart, Marcelo; Kuhn, Martin; Martini, Paul; Chen, Lei; Hagelberg, Frank; Kaiser, Alexander; Scheier, Paul; and Ellis, Andrew M.. 2018. Highly Stable [C₆₀AuC₆₀]^{+/-} Dumbbells. *Journal of Physical Chemistry Letters*. Vol.9(10). 2703-2706. <https://doi.org/10.1021/acs.jpcclett.8b01047> PMID: 29722981

This Article is brought to you for free and open access by the Faculty Works at Digital Commons @ East Tennessee State University. It has been accepted for inclusion in ETSU Faculty Works by an authorized administrator of Digital Commons @ East Tennessee State University. For more information, please contact digilib@etsu.edu.

Highly Stable [C₆₀AuC₆₀]^{+/-} Dumbbells

Copyright Statement

This is an open access article published under a Creative Commons Attribution (CC-BY) License, which permits unrestricted use, distribution and reproduction in any medium, provided the author and source are cited.

Creative Commons License



This work is licensed under a [Creative Commons Attribution 4.0 International License](https://creativecommons.org/licenses/by/4.0/).

Creator(s)

Marcelo Goulart, Martin Kuhn, Paul Martini, Lei Chen, Frank Hagelberg, Alexander Kaiser, Paul Scheier, and Andrew M. Ellis

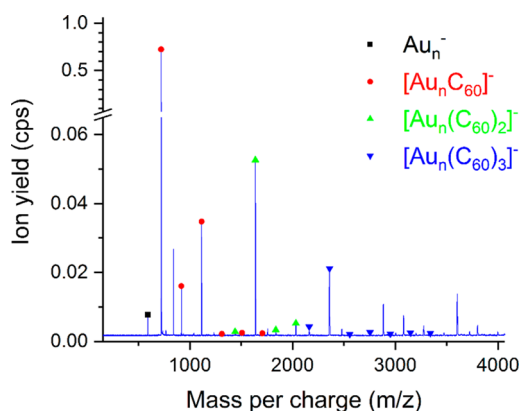


Figure 1. Mass spectrum of $[\text{Au}_n(\text{C}_{60})_m]^-$ anions. Note that only one bare Au_n^- ion, Au_3^- , is visible in this image. Note also that for the series of peaks identified as coming from $[\text{Au}_n\text{C}_{60}]^-$, $[\text{Au}_n(\text{C}_{60})_2]^-$, and $[\text{Au}_n(\text{C}_{60})_3]^-$, each series begins at $n = 1$.

almost completely dominates. There is a similar dominance for $[\text{Au}(\text{C}_{60})_3]^-$ in the $m = 3$ series.

We can also identify anomalous intensity behavior for the cations, as can be seen in Figure 2. In the $[\text{Au}_n\text{C}_{60}]^+$ series, the

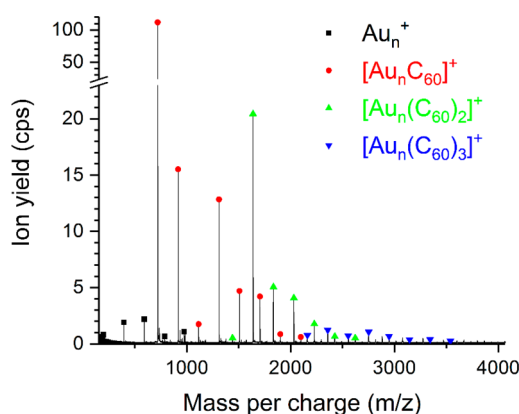


Figure 2. Mass spectrum of $[\text{Au}_n(\text{C}_{60})_m]^+$ cations. For the series of peaks identified as coming from $[\text{Au}_n\text{C}_{60}]^+$, $[\text{Au}_n(\text{C}_{60})_2]^+$, and $[\text{Au}_n(\text{C}_{60})_3]^+$, note that each series begins at $n = 1$.

$[\text{Au}_2\text{C}_{60}]^+$ ions have an abnormally low abundance and, therefore, show antimagic behavior. Similar to the anions, although not quite so extreme, the $[\text{Au}(\text{C}_{60})_2]^+$ ion is dominant in the $[\text{Au}(\text{C}_{60})_m]^+$ series. We can therefore conclude that $[\text{Au}(\text{C}_{60})_2]^{+/-}$ ions are particularly stable ions regardless of charge state.

To try and explain these findings, we have performed density functional theory (DFT) calculations, as detailed in the Supporting Information. These calculations have been used to predict dissociation energies of the ions, which are shown in Table 1. Where there is more than one possible dissociation channel, only the dissociation energy for the lowest-energy channel is shown. The calculations have been restricted to complexes with a maximum of two C_{60} molecules in order to keep the calculations affordable. We find good agreement between the theoretical predictions and our experimental findings. For example, the energy needed to remove one C_{60} molecule from $[\text{Au}(\text{C}_{60})_2]^-$ is considerably higher than that for $[\text{Au}_2(\text{C}_{60})_2]^-$, which is consistent with the magic character of the former when compared with the latter. Likewise, the

Table 1. Calculated Dissociation Energies of $[\text{Au}_n(\text{C}_{60})_m]^{+/-}$ Ions

complex	dissociation products ^a	dissociation energy/eV
$[\text{AuC}_{60}]^+$	$\text{Au} + \text{C}_{60}^+$	1.38
$[\text{Au}_2\text{C}_{60}]^+$	$\text{Au}_2 + \text{C}_{60}^+$	0.79
$[\text{Au}_3\text{C}_{60}]^+$	$\text{Au}_3^+ + \text{C}_{60}$	1.72
$[\text{Au}(\text{C}_{60})_2]^+$	$\text{AuC}_{60} + \text{C}_{60}^+$	1.47 ^b
$[\text{Au}_2(\text{C}_{60})_2]^+$	$\text{Au}_2\text{C}_{60} + \text{C}_{60}^+$	1.05 ^b
$[\text{AuC}_{60}]^-$	$\text{Au} + \text{C}_{60}^-$	0.83
$[\text{Au}_2\text{C}_{60}]^-$	$\text{Au}_2 + \text{C}_{60}^-$	0.98
$[\text{Au}_3\text{C}_{60}]^-$	$\text{Au}_3^- + \text{C}_{60}$	0.49
$[\text{Au}(\text{C}_{60})_2]^-$	$\text{AuC}_{60} + \text{C}_{60}^-$	0.83
$[\text{Au}_2(\text{C}_{60})_2]^-$	$\text{Au}_2\text{C}_{60} + \text{C}_{60}^-$	0.51 ^b

^aOther dissociation products are possible (see the Supporting Information), but those listed in this column are the calculated lowest-energy dissociation channels. ^bOptimized structures with a few low-lying imaginary frequencies. In these cases, zero-point corrections were not taken into account.

enhanced abundance of $[\text{Au}_2\text{C}_{60}]^-$ relative to $[\text{AuC}_{60}]^-$ is explicable in terms of the calculated dissociation energies. In the case of cations, the $[\text{Au}_2\text{C}_{60}]^+$ ion has a far lower dissociation energy than either $[\text{AuC}_{60}]^+$ or $[\text{Au}_3\text{C}_{60}]^+$, explaining the weak $[\text{Au}_2\text{C}_{60}]^+$ peak in the mass spectrum. Given this good agreement between theory and experiment, we feel that the current calculations capture the essence of the Au– C_{60} interactions.

The mass spectra clearly demonstrate new ion chemistry resulting from the interaction between Au and C_{60} . One is particularly drawn to the strongly magic character associated with the $[\text{Au}(\text{C}_{60})_2]^{+/-}$ ions, and it is tempting to draw parallels with other well-known $[\text{AuX}_2]^{+/-}$ ions.^{6–9,19} The DFT calculations predict that the two C_{60} molecules are located on opposite sides of the Au atom in a dumbbell-like arrangement, as illustrated pictorially in Figure 3. The Mulliken charges on

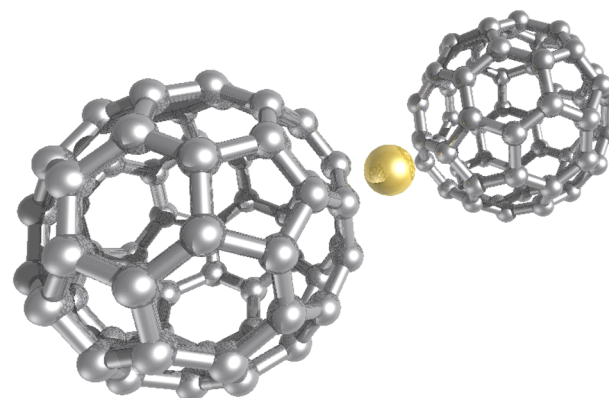


Figure 3. Calculated lowest-energy structure of $[\text{Au}(\text{C}_{60})_2]^+$.

the Au atom are +0.59 and +0.38 for the cation and anion, respectively, i.e., in both cases the metal center is positively charged. The ionization energy of C_{60} is considerably lower than that of Au, and therefore, one might expect the majority of the positive charge in the cation to reside on the C_{60} molecules. The fact that this is quite different from the Mulliken prediction suggests a significant covalent component to the bonding, as posited previously for other $[\text{AuX}_2]^+$ ions.^{6,7}

Likewise, the higher electron affinity of C_{60} (2.68 eV)²¹ when compared with that of a gold atom (2.31 eV)²² should draw

much of the excess negative charge in $[\text{Au}(\text{C}_{60})_2]^-$ toward the C_{60} molecules. However, the Mulliken analysis suggests that this anion is some way from being described as $\text{C}_{60}^{-0.5}\text{AuC}_{60}^{-0.5}$: further charge transfer from the Au occurs, creating an electron-deficient Au atom. The calculated charge on the Au atom is similar to that calculated for anions such as $[\text{Au}(\text{CN})_2]^-$ and $[\text{AuCl}_2]^-$, where substantial contributions from both ionic and covalent bonding have been found.^{8,9} It is likely that the binding in $[\text{Au}(\text{C}_{60})_2]^-$ is of a similar mixed composition.

To explore this further, we show in Figure 4a a calculated charge density difference map obtained at the optimized structure for $[\text{Au}(\text{C}_{60})_2]^+$. This image indicates that there is a small amount of charge accumulation in the form of two small blue lobes between the closest C and Au atoms. Figure 4b shows a contour plot of the electron localization function (ELF)²³ near to the Au atom. The ELF between adjacent

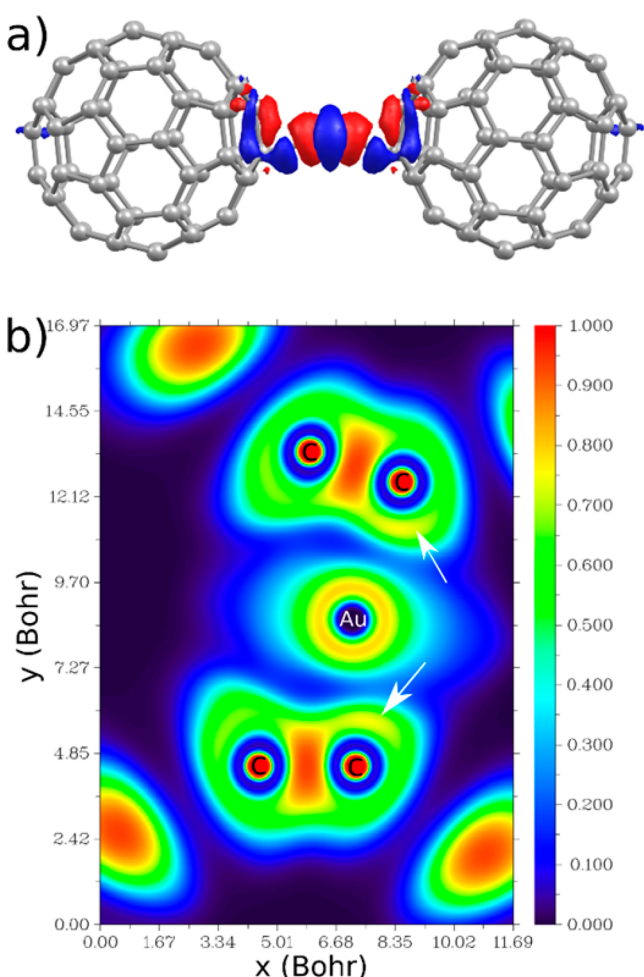


Figure 4. (a) Calculated charge density difference map for $[\text{Au}(\text{C}_{60})_2]^+$ fixed at its equilibrium geometry. This image shows the isosurface (isovalue $0.002608 \text{ e}/a_0^3$) of the charge density difference $\rho([\text{Au}(\text{C}_{60})_2]^+) - \rho((\text{C}_{60})_2^+) - \rho(\text{Au})$. Blue regions indicate charge accumulation, and red regions indicate charge depletion. (b) Contour map of the electron localization function (ELF) in the region close to the Au atom, as calculated with the multiwfn utility program.²⁰ The dumbbell is vertically oriented in this plot, and the plane cuts through the gold atom of $[\text{Au}(\text{C}_{60})_2]^+$ and four neighboring C atoms. The white arrows point to zones between the Au atom and the nearest C atoms in each C_{60} molecule where $\text{ELF} \approx 0.75$.

carbon atoms has a value close to 1.0, showing (as expected) that these are strongly covalent bonds. An arc (indicated by white arrows) with $\text{ELF} \approx 0.75$ lies between the Au atom and the closest C atom in each C_{60} molecule, which indicates some covalent bonding. Very similar conclusions can be drawn for the anion. We note that the calculated distance between the Au atom and the nearest carbon atom in the $[\text{Au}(\text{C}_{60})_2]^-$ anion is 2.216 \AA , which is significantly longer than the Au–C distances reported for $[\text{Au}(\text{CN})_2]^-$ (1.99 \AA)⁸ and $[\text{AuC}_2]^-$ (1.95 \AA).²⁴

The discovery of $[\text{C}_{60}\text{AuC}_{60}]^{+/-}$ ions with stable dumbbell structures in the gas phase suggests the possibility that these complexes, and particularly the anion, might be synthesized in conventional wet chemistry. Such ions are new to chemistry and may prove to be useful tools in both gold and fullerene chemistry. Although not included in the current study, we flag the possibility that the corresponding neutral dumbbell species may also show particular stability. The applications of complexes built from these components are not clear at this juncture, but possibilities may exist in the development of new supramolecular architectures involving fullerenes. The potential also exists in molecular electronics given the ongoing interest in gold–fullerene contacts in nanoelectronics.^{10–14} We therefore hope that the current study prompts a search for the $\text{C}_{60}\text{AuC}_{60}$ dumbbell moiety, both in solution chemistry and in the solid state.

■ ASSOCIATED CONTENT

Supporting Information

The Supporting Information is available free of charge on the ACS Publications website at DOI: [10.1021/acs.jpcllett.8b01047](https://doi.org/10.1021/acs.jpcllett.8b01047).

Computational methodology employed; calculated ionization energies and electron affinities; and calculated dissociation energies for various ions (PDF)
Structural information for the species studied (ZIP)

■ AUTHOR INFORMATION

Corresponding Authors

*E-mail: paul.scheier@uibk.ac.at (P.S.).

*E-mail: andrew.ellis@le.ac.uk (A.M.E.).

ORCID

Alexander Kaiser: 0000-0002-9439-9176

Paul Scheier: 0000-0002-7480-6205

Andrew M. Ellis: 0000-0001-7456-9214

Notes

The authors declare no competing financial interest.

■ ACKNOWLEDGMENTS

This work was supported by the Austrian Science Fund FWF (Projects P26635, M1908, and P28979-N27) and the European Commission (ELEvaTE H2020 Twinning Project).

■ REFERENCES

- (1) Pyykkö, P. Theoretical Chemistry of Gold. *Angew. Chem., Int. Ed.* **2004**, *43*, 4412–4456.
- (2) Wang, L. – S. Covalent gold. *Phys. Chem. Chem. Phys.* **2010**, *12*, 8694–8705.
- (3) Teles, J. H.; Brode, S.; Chabanas, M. Cationic Gold(I) Complexes: Highly Efficient Catalysts for the Addition of Alcohols to Alkynes. *Angew. Chem., Int. Ed.* **1998**, *37*, 1415–1418.
- (4) Gorin, D. J.; Toste, F. D. Relativistic effects in homogeneous gold catalysis. *Nature* **2007**, *446*, 395–403.

(5) Hunks, W. J.; Jennings, M. C.; Puddephatt, R. J. Supramolecular Gold(I) Thiobarbiturate Chemistry: Combining Auophilicity and Hydrogen Bonding to Make Polymers, Sheets, and Networks. *Inorg. Chem.* **2002**, *41*, 4590–4598.

(6) Pyykkö, P. Predicted Chemical Bonds between Rare Gases and Au⁺. *J. Am. Chem. Soc.* **1995**, *117*, 2067–2070.

(7) Xin-Ying, L.; Xue, C. *Ab initio* study of MXe_n⁺ (M = Cu, Ag, and Au; n = 1,2). *Phys. Rev. A: At., Mol., Opt. Phys.* **2008**, *77*, 022508.

(8) Wang, X. – B.; Wang, Y. – L.; Yang, J.; Xing, X. – P.; Li, J.; Wang, L. – S. Evidence of Significant Covalent Bonding in Au(CN)₂⁻. *J. Am. Chem. Soc.* **2009**, *131*, 16368–16370.

(9) Xiong, X. – G.; Wang, Y. – L.; Xu, C. – Q.; Qiu, Y. – H.; Wang, L. – S.; Li, J. On the gold–ligand covalency in linear [AuX₂]⁻ complexes. *Dalton Trans.* **2015**, *44*, 5535–5546.

(10) Joachim, C.; Gimzewski, J. K.; Schlittler, R. R.; Chavy, C. Electronic Transparency of a Single C₆₀ Molecule. *Phys. Rev. Lett.* **1995**, *74*, 2102–2105.

(11) McEuen, P. L.; Park, H.; Park, J.; Lim, A. K.; Anderson, E. H.; Alivisatos, A. P. Nanomechanical oscillations in a single-C₆₀ transistor. *Nature* **2000**, *407*, 57–60.

(12) Parks, J. J.; Champagne, A. R.; Hutchison, G. R.; Flores-Torres, S.; Abruña, H. D.; Ralph, D. C. Tuning the Kondo Effect with a Mechanically Controllable Break Junction. *Phys. Rev. Lett.* **2007**, *99*, 026601.

(13) Yee, S. K.; Malen, J. A.; Majumdar, A.; Segalman, R. A. Thermoelectricity in Fullerene–Metal Heterojunctions. *Nano Lett.* **2011**, *11*, 4089–4094.

(14) Bilan, S.; Zotti, L. A.; Pauly, F.; Cuevas, J. C. Theoretical study of the charge transport through C₆₀-based single-molecule junctions. *Phys. Rev. B: Condens. Matter Mater. Phys.* **2012**, *85*, 205403.

(15) Lyon, J. T.; Andrews, L. Infrared Spectrum of the Au–C₆₀ Complex. *ChemPhysChem* **2005**, *6*, 229–232.

(16) Shukla, M. K.; Dubey, M.; Leszczynski, J. Theoretical investigation of electronic structures and properties of C₆₀-gold nanocontacts. *ACS Nano* **2008**, *2*, 227–234.

(17) Zeng, Q.; Chu, X.; Yang, M.; Wu, D. – Y. Spin–orbit coupling effect on Au–C₆₀ interaction: A density functional theory study. *Chem. Phys.* **2012**, *395*, 82–86.

(18) Soler, J. M.; Sáenz, J. J.; García, N.; Echt, O. The effect of ionization on magic numbers of rare-gas clusters. *Chem. Phys. Lett.* **1984**, *109*, 71–75.

(19) Schröder, D.; Brown, R.; Schwerdtfeger, P.; Wang, X. B.; Yang, X.; Wang, L. S.; Schwarz, H. Gold Dichloride and Gold Dibromide with Gold Atoms in Three Different Oxidation States. *Angew. Chem., Int. Ed.* **2003**, *42*, 311–314.

(20) Lu, T.; Chen, F. Multiwfn: A multifunctional wavefunction analyzer. *J. Comput. Chem.* **2012**, *33*, 580–592.

(21) Huang, D. L.; Dau, P. D.; Liu, H. – T.; Wang, L. S. High-resolution photoelectron imaging of cold C₆₀⁻ anions and accurate determination of the electron affinity of C₆₀. *J. Chem. Phys.* **2014**, *140*, 224315.

(22) Wu, X.; Qin, Z. B.; Xie, H.; Cong, R.; Wu, X. H.; Tang, Z. C.; Fan, H. J. Photoelectron Imaging and Theoretical Studies of Group 11 Cyanides MCN (M = Cu, Ag, Au). *J. Phys. Chem. A* **2010**, *114*, 12839–12844.

(23) Silvi, B.; Savin, A. Classification of chemical bonds based on topological analysis of electron localization functions. *Nature* **1994**, *371*, 683–686.

(24) León, I.; Yang, Z.; Wang, L. – S. Probing the electronic structure and Au–C chemical bonding in AuC₂⁻ and AuC₂ using high-resolution photoelectron spectroscopy. *J. Chem. Phys.* **2014**, *140*, 084303.